JOURNAL OF Materials CHEMISTRY

Hydrothermal deposition of small α-Fe_2O_3 (hematite) particles on ordered zirconium phosphonate multilayer SAMs on gold

Marc Nagtegaal, Jörg Küther, Jürgen Ensling, Philipp Gütlich and Wolfgang Tremel

Institut für Anorganische Chemie und Analytische Chemie, Johannes Gutenberg-Universität, Mainz Becher Weg 24, Mainz D-55099, Germany. E-mail: tremel@indigotrem1.chemie.uni-mainz.de

Received 30th November 1998, Accepted 21st January 1999

We present the use of self-assembled monolayers of Zr–phosphonate multilayers (bilayers in terms of metal atoms) as substrates for the heterogeneous nucleation of hematite under hydrothermal conditions. The phosphonate multilayers display high (hydro)thermal stability which we establish beforehand. The films of the hematite nanoparticles have been characterised using techniques including atomic force microscopy and Mössbauer spectroscopy in reflection. This latter technique shows up the effect of the small particle sizes of the hematite particles on the nature of the magnetic ordering.

1 Introduction

Recent studies have shown that two-dimensional organic interfaces such as self-assembled monolayers (SAMs) of substituted alkylsilanes and modified polymer surfaces are effective in controlling the nucleation of iron oxides and oxide–hydroxides from aqueous solutions.[1] An interesting aspect of these studies is the very specific nature of the nucleation; only when the organic surfaces are specially modified (for example by sulfonate functionalities) do the iron compounds nucleate. Unmodified polymer surfaces, for example, of polyethylene, are unable to provide the initial interaction between the surface and the nucleating inorganic material for the precipitation to take place. Our own studies have been aimed at the use of ω-substituted alkylthiol SAMs on gold surfaces for the heterogenous nucleation of the iron oxide–hydroxide lepidocrocite [γ-FeO(OH)] from solutions of Fe(III) *below* supersaturation. By this, we mean that, left to themselves, the Fe(III) solutions might be stable for weeks, but the insertion of SAMs with suitable ω-substituents results in the formation of films of lepidocrocite within periods of hours. *In situ* investigations by surface plasmon spectroscopy (SPS) confirm the specificity of the nucleation. At the solution pH used by us, lepidocrocite forms only when the ω-substituent on the thiol SAM is the sulfonate group.[2]

A factor limiting the use of SAMs for the nucleation of minerals from solution is their low thermal stability. SAMs of thiols on gold surfaces desorb or decompose at elevated temperatures.[3] Metal–phosphonate multilayers, first prepared by Mallouk and coworkers[4] offer greater thermal stability than SAMs built up from alkyl thiols. These systems have been used to template the growth of oriented molecular sieve crystals[5] and for the attachment of zeolite crystals.[6] Hydrothermal synthesis offers an important route to iron oxide materials.[7] Recent studies have extended the use of hydrothermal techniques to the synthesis of thin iron oxide films on silicon surfaces.[8] The advantages of hydrothermal preparation techniques include the relatively simple experimental setup and the low temperature of preparation. The harsh conditions typical of hydrothermal synthesis however preclude the use of SAMs of the usual long chain thiols on Au(111) surfaces. To exploit the control over nucleation offered by SAM substrates under hydrothermal conditions, it is important to find thermally stable SAMs.

In this contribution we shall first establish the formation and (hydro)thermal stability of zirconium phosphonate multilayers (usually bilayers in terms of the metal atom) using surface plasmon spectroscopy (SPS). We shall then use hydrothermal techniques to nucleate the formation of the important iron oxide hematite (α-Fe_2O_3) on these surfaces. In using these hydrothermal conditions, we follow routine procedures for the preparation of hematite.[9] The difference is that we are able to deposit films of hematite on SAMs. The iron oxide films have been characterised by techniques including atomic force microscopy (AFM) and Mössbauer spectroscopy.

Thin iron oxide films have been synthesized using a variety of techniques such as sputtering,[10] pulsed laser evaporation,[11] chemical vapor deposition[12] and spray pyrolysis.[13] Interest in such thin films arises from a variety of applications in the electronics industry, corrosion proofing and as magnetic pigments.[9] Hematite itself is an important magnetic material and as such, its preparation as thin films under rather mild conditions is of considerable interest.

2 Experimental

Solutions of aqueous Fe(III) nitrate solutions were prepared from $Fe(NO)_3{\cdot}9H_2O$ (99.99%) (Aldrich) and deionized water (18.3 MΩ cm^{-1}, Barnsted, Easypure). 11-mercaptoundecan-1-ol (MUDO), $HO(CH_2)_{11}SH$ was prepared *via* the Bunte salt.[14] 1,10-decandiylbis(phosphonic acid) (DBP), $H_2O_3P(CH_2)_{10}PO_3H_2$ and undecanmonophosponate (UMP), $H_2O_3P(CH_2)_{10}CH_3$ were prepared following the reported procedure of Mallouk and coworkers[15] from 1,10-dibromodecane or 1-bromoundecane (Aldrich 97%) and triethyl phosphite (Aldrich, 98%) with subsequent hydrolysis using HCl. Phosphonate multilayers were prepared by the adsorption of mercaptoundecanol on gold(111) surfaces followed by phosphorylation with $POCl_3$ (Merck >99%) and 2,4,6-collidine (Fluka >99%) in acetonitrile (Merck GR dried).[16–18] 48 nm gold films were evaporated on cleaned glass slides (B270) after an initial layer of 2–3 nm Cr was first deposited to increase the adhesion, in a Balzers, Baltec evaporation chamber. The evaporation was carried out with a rate of 0.1 nm s^{-1} and a pressure of 5×10^{-6} mbar. Self-assembled monolayers of MUDO were adsorbed onto Au by placing the substrates in ethanolic solutions of MUDO for 12–15 h. After the adsorption, the substrates were washed with ethanol to remove unbound thiols. The monolayers were phosphorylated for 1 h in a solution of 0.2 M phosphorous oxychloride ($POCl_3$) and 2,4,6-collidine in dry acetonitrile under a N_2 atmosphere. Phosphonate multilayers were then produced with successive adsorption by alternate exposure to aqueous solutions of

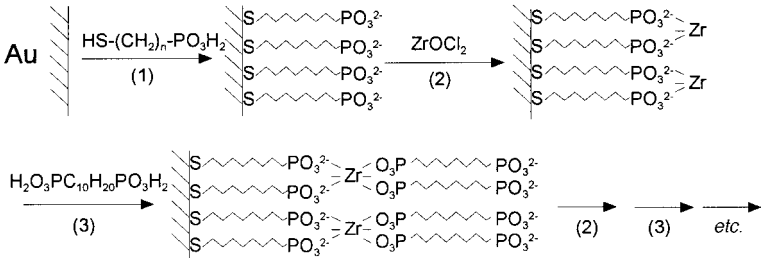

Scheme 1

5 mM zirconyl chloride octahydrate $ZrOCl_2 \cdot 8H_2O$ and 1.2 mM solutions of 1,10-decandiylbis(phosphonic acid) (DBP) each for 30 min (Scheme 1). Between each step, the substrates were thoroughly rinsed with water and blown dry with nitrogen. The use of UMP in the last absorption step under the same conditions used for DBP resulted in the production of hydrophobic substrates which were used to compare the effect of phosphonate and methyl termination on the multilayer SAM. All the multilayers used contained two layers of Zr^{4+}.

The hydrothermal preparation of hematite, α-Fe_2O_3 was achieved *via* hydrolysis of 0.02 M solutions of iron(III) nitrate (pH = 2.34). Reactions were carried out in a modified Teflon cuvette shown schematically in Fig. 1. The functionalized glass slides were placed face down in the chamber into the solution. The Teflon cuvette had a volume of 35 mL and was filled with 15 mL of the solution. All reactions were performed under hydrothermal conditions at 180 ± 1 °C for 1 h in a thermostat controlled oven. Thicker films, especially for X-ray mesurements were formed by repeated addition of fresh iron(III) solution.

Contact angle measurements on the SAMs against water were performed using a Krüss G1 microscope. Advancing angles were taken with fresh milipore water at three different points on the substrates. FTIR spectra were used to monitor the multilayer formation. The spectra were taken using a Nicolet 5DXC spectrometer with a Spectratech FT80 Specular Reflectance attachment, employing an incident angle of 85° to the normal. The assembly and thermal stability of the phosphonate multilayers was monitored with surface plasmon spectroscopy in the Kretschmann configuration.[19,20] Optical coupling was achieved with a LASFN9 prism ($n = 1.85$ at $\lambda =$ 623.8 nm) and an index matching fluid ($n = 1.70$) between the prism and the BK270 glass slide of index. The incident light source was a He–Ne laser ($\lambda = 623.8$ nm, power = 5 mW). The precipitates were collected from the surface and stuck to Scotchtape™ for powder X-ray measurements in the transmission mode using a Siemens D5000 powder diffractometer equipped with Ge(111) monochromatized Cu-Kα radiation ($\lambda = 1.54056$ Å) in $\theta/2\theta$ transmission geometry. The data set was acquired from 20 to 50° in 2θ with a step size of 0.03° and a time of 55 s per step. Transmission FTIR of the iron oxide powders in pressed KBr pellets were acquired on a Mattson Instruments spectrometer. For acquiring the Mössbauer spectra, we employed integral conversions electron Mössbauer spectroscopy (ICEMS). This is a very surface sensitive technique that allows thin films to be studied. Typical surface penetration is of the order of 300 nm. The converted electron from the Mössbauer resonance process is detected using a proportional counter filled with a He–CH_4 (96%–4%) mixture. Atomic force microscopy (AFM) was used to investigate crystal morphologies of the freshly prepared particles. The samples were examined using a Nanoscope IIIa in tapping mode using silicon cantilevers and a scan rate of 0.5 Hz.

3 Results and discussion

3.1 Formation and thermal stability of zirconium phosphonate multilayers on gold

The layer by layer growth of organophosphonate multilayers was followed using surface plasmon spectroscopy (Fig. 2). The spectra show a continous shift of the plasmon curves after each adsorption step. Using the Fresnel formula for the shift in the plasmon curves as a function of the thickness, we obtain from curves such as the ones shown, the result that each ZrP layer is *ca.* 17 Å thick. We are unable to simultaneously determine the refractive index and the thickness of a thin film using SPS operating with a single wavelength excitation. For

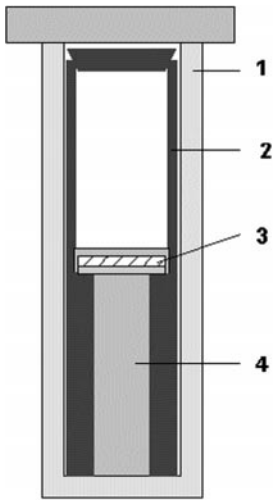

Fig. 1 Autoclave lined with a modified Teflon cuvette. The labels refer to: 1, the hydrothermal steel bomb; 2, the Teflon cuvette; 3, the ZrP multilayer coated gold-glass substrate; 4, is the Fe(III) solution.

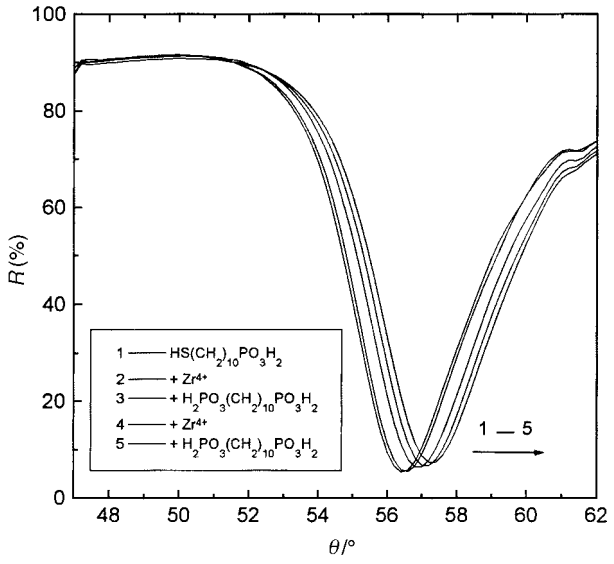

Fig. 2 SPS traces following the formation of the metal–phosphonate multilayers. The various traces correspond to the steps described in the figure.

this reason, it was necessary to assume the refractive index of Zr^{4+} to be 1.5. The thickness obtained is consistent with published ellipsometry results.[4,15] Contact angle measurements also support the picture of the alternate assembly of the phosphonate layer and Zr^{4+} ions; the angles alternating between high and low values (Table 1). We observe that the contact angle of a double Zr/DBP layer is higher than from the phosphonate monolayer. This might due to incomplete phosphorylation process of the initial MUDO monolayer with $POCl_3$. The value for the double layer is however compatible with published data [$\theta_a(H_2O) = 70$[21]] and therefore we suggest that if the phosphorylation of the initial MUDO SAM is poor, it is compensated in the later stages of the multilayer formation. FTIR specular reflectance spectra of the final assembly are shown in Fig. 3 and are dominated by the asymmetric phosphonate stretch in the mid-IR region at 1077 cm^{-1} (the reference value[16] is 1076 cm^{-1}).

Initial attempts to use normal alkylthiol SAMs under hydrothermal conditions failed; under the conditions mentioned in the experimental section, SAMs of long-chain thiols were visibly damaged after removal from the hydrothermal chamber. This was also true of clean gold substrates. For the ZP multilayers, such damage was not noted and the stability was monitored with SPS. Samples of the prepared phosphonate multilayers on gold showed no change of the plasmon reflectivity before and after the reaction of these films under hydrothermal conditions for 1 h at 180 °C (Fig. 4). This indicates a high degree of thermal stability of the ZrP multilayers under hydrothermal treatment.

3.2 Hydrothermal deposition of hematite α-Fe_2O_3 on the multilayers

The hydrolysis of iron(III) nitrate solutions at 180 °C in an autoclave permits the formation of hematite α-Fe_2O_3 within a 1 h reaction time.[22] Concentrations of 1 and 0.1 M iron(III) nitrate allow *homogeneous* precipitates to be formed in solution. No homogeneous precipitate was obtained when the concentrations were lower than 0.02 M. However, even at this concentration, the colour of the solution changes and the pH drops indicating the formation of polynuclear complexes through partial hydrolysis,[23] and material is deposited through *heterogeneous* nucleation on the multilayer SAM substrate. With time, under the hydrothermal conditions for pure *heterogeneous* precipitation, *viz.* concentrations below 0.02 M, we observe a change of colour on the substrate from gold to orange, indicating an influence of the modified surface on the heterogeneous nucleation of iron oxide films. The phosphonate group is not very acidic and at the working pH of 2.34 it is not predicted to be a strongly complexing agent for iron ions in 'normal solutions'. However, the hydrothermal process seems to promote heterogeneous nucleation. The influence of diphosphonates in the tailored synthesis of iron oxides from 0.02 M iron(III) chloride at pH = 2 has been examined by Reeves and Mann.[24]

When the CH_3-terminated Zr/UMP multilayers were used instead of the phosphonate-terminated surfaces, very little material deposited on the substrates. The material so deposited could be easily washed away, unlike on the phosphonate-terminated surface, and through SPS measurements, the complete absence of material could be confirmed. Their high thermal stability has made the phosphonate multilayer systems suitable for the preparation of iron oxides under hydrothermal conditions.

Table 1 Contact angles after intermediate steps in the growth of metal–phosphonate multilayers

Surface	θ_a (H_2O)
Au	59
Au/SH$(CH_2)_{10}$OH	17
Au/SH$(CH_2)_{11}PO_3H_2$	47
Au/SH$(CH_2)_{10}PO_3$/Zr	14
Au/SH$(CH_2)_{10}PO_3$/Zr/$H_2PO_3(CH_2)_{10}PO_3H_2$	65
Au/SH-$(CH_2)_{10}PO_3$/Zr/$H_2PO_3(CH_2)_{10}CH_3$	116

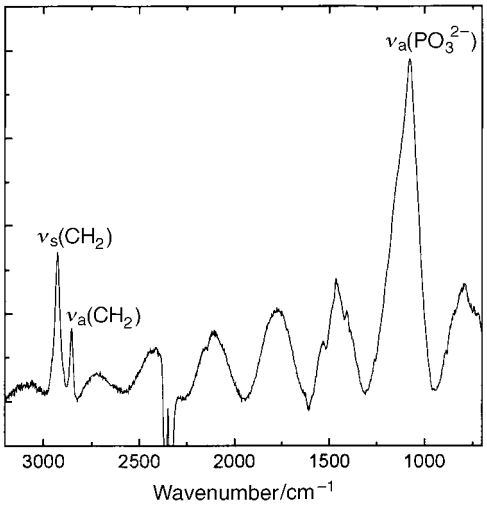

Fig. 3 FTIR spectrum obtained in specular reflectance of a zirconium/phosphonate double layer on gold. The spectrum shows the asymmetric phosphonate stretch. The broad fringes in the background are caused by interference and do not correspond to vibrations.

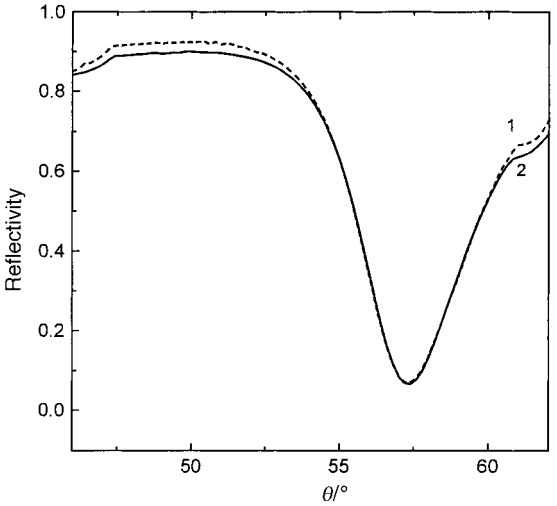

Fig. 4 SPS traces attesting to the thermal stability of the metal phosphonate multilayer. Trace 1 corresponds to the multilayer substrate before exposure to hydrothermal conditions. Trace 2 was acquired after 1 h in the hydrothermal chamber as described in the text. The traces overlap almost perfectly.

3.3 Characterisation of the material

In the binary and ternary Fe–O–H systems, there are as many as 18 crystalline phases.[9] It is therefore of some importance to establish unambiguously, the nature of the crystalline phases formed. Collection of the powders from as many as five multilayer surfaces after the hydrothermal preparations, with the Fe(III) solutions being refreshed as many as five times permitted sufficient material to be obtained for a complete characterisation by powder X-ray diffraction. A search of the JCPDS files suggested that hematite was the only phase present.

This was further confirmed through Rietveld refinement of the powder diffraction data using the XND program.[25] The experimental data and the fitted profile are displayed in Fig. 5. The poor crystallinity of the material resulted in rather broad

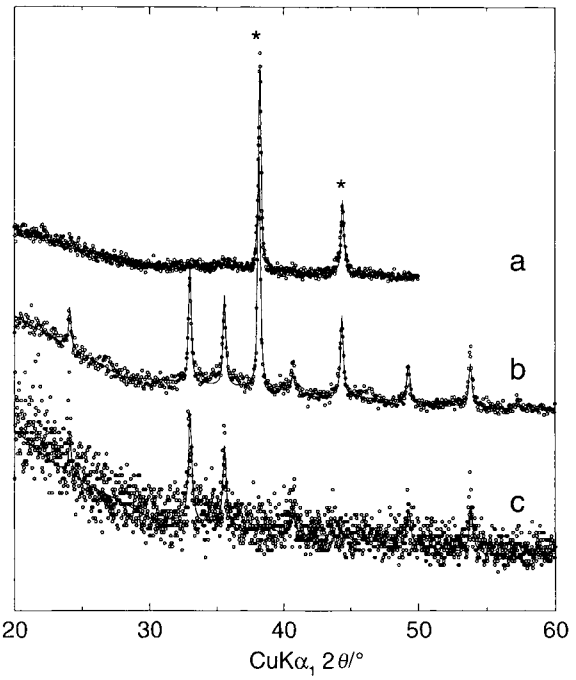

Fig. 5 X-Ray powder diagram of the hematite precipitate obtained on Zr/DBP multilayer substrates a and as homogeneous precipitates c under hydrothermal conditions. The data and the Rietveld fit are displayed. The asterisks mark peaks from gold. Pattern b displays the experimental profile and the Rietveld fit of sample a after it was aged at the room temperature for two months. The peaks are narrower and the sample is more crystalline due to the particles having grown larger.

peaks so the data obtained initially were not very convincing. However, aging the samples at the room temperature for a period of two months resulted in significant growth in the particle size and improvement in the X-ray crystallinity. The different traces in Fig. 5 attest to this. Additional characterisation was obtained from transmission IR spectroscopy on the powders and is presented in Fig. 6. The IR absorption bands correspond to the expectation from literature.[9]

3.3 Mössbauer spectroscopy

Fig. 7 displays the Mössbauer reflection (ICEMS) spectra of the hematite films obtained at room temperature. Three subspectra c, d and e were used to successfully fit the data (the sum is the trace b). The subspectra c correspond to particles

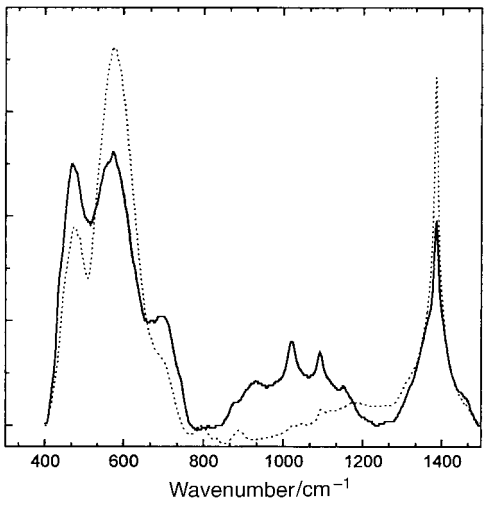

Fig. 6 (a) FTIR in transmission (KBr pellets) of the hematite powder obtained on Zr/DBP multilayer substrates (straight line) and of hematite obtained from homogeneous precipitation (dotted line).

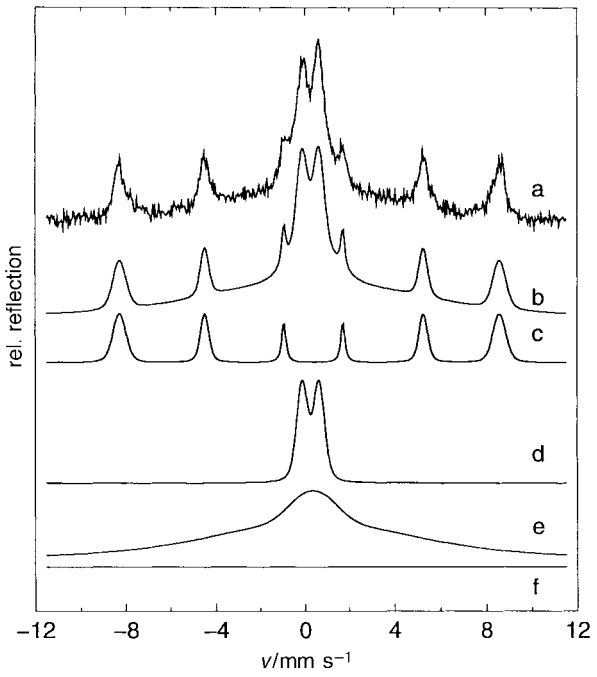

Fig. 7 Experimental and fitted Mössbauer reflection spectra of hematite films grown hydrothermally on Zr/DBP multilayer substrates. a is the experimental spectrum (referenced to α-Fe), b is the sum of the subspectra c, d and e, f is the background.

that are large enough to create a sextet, d due to small superparamagnetic particles and e arises from particles whose sizes are between the two other subspectra. This was despite there being no evidence from the isomer shifts and the quadrupole splittings for any other species than hematite.

3.4 Atomic force microscopy

Hematite has the same crystal structure type as corundum,[26] comprising nearly hexagonal close-packed oxide ions with Fe(III) in the interstitial octahedral sites. Following Megaw,[26] we can describe the structure as comprising pairs of octahedra sharing faces parallel to the *c* axis of the structure. Each octahedron is linked through edges to three others in its plane. The structure is shown in Fig. 8(a) in a projection down [110] (or [11$\bar{2}$0] using the *hkil* notation). If we consider any of the oxygen sheets parallel to the *ab* plane, (say at $z=0.16667$), we see that it can be described as constructed from triangles of oxygen with a side of *ca.* 2.7 Å, each arranged in a hexagonal close-packed manner. These are shown in Fig. 8(b). These triangles of oxygen are actually define the shared faces between the metal–oxygen octahedra. The separation between the centres of the triangles is about 5 Å. If the terminal phosphonate groups in the multilayer were arranged as in a normal SAM such as hexadecanethiol,[27] then there could be nearly perfect epitaxy between the P of the phosphonate groups (which would be arranged in a hexagonal lattice with a constant spacing of *ca.* 5 Å) and the triangles of oxygen ions of the α-Fe_2O_3 sheet. For the multilayers used here, we might expect a larger spacing than 5 Å between the headgroups but the possibility of such near-epitaxial templating remains. Additionally, the O···O separation of 2.7 Å within the triangles is very close to the O···O separation in organic phosphates.[24] This discussion provides us some basis to discuss the AFM images. That hematite crystallizes in a rhombohedral space group without being layered in any sense suggests that the morphology would tend to be isotropic.

Fig. 9 displays a tapping mode AFM image of the phosphonate multilayer SAM on gold-glass in low magnification. This image helps to establish the features on the substrate so that any material grown on them may be easily

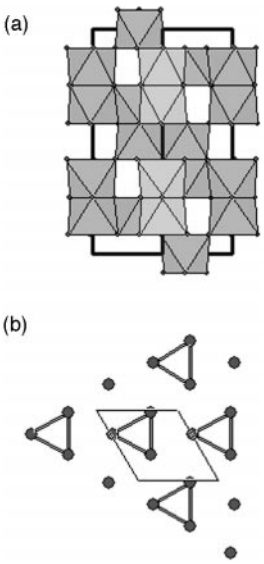

Fig. 8 (a) Structure of α-FeO(OH) hematite in a projection down [110] (or [11$\bar{2}$0]) showing the double FeO_6 octahedra sharing faces along [001] (or [0001]). (b) View down [0001] of a single nearly close-packed sheet of oxygen in the hematite structure. The O atoms cluster in triangles with an edge of 2.7 Å. The centers of the triangles are arranged on a hexagonal lattice with a spacing of around 5 Å.

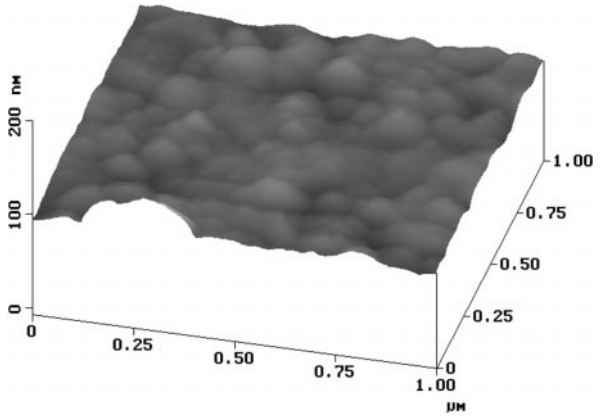

Fig. 9 Surface view tapping mode AFM image of a Zr/DBP multilayer surface on gold-glass.

discriminated. The pair of images in Fig. 10 display height and amplitude tapping mode images of a typical substrate after a single hydrothermal run [without refreshing of Fe(III) solution]. The material is seen to have deposited evenly and appears homogeneous in the manner in which individual particles extend in the plane of the substrate. A surface view

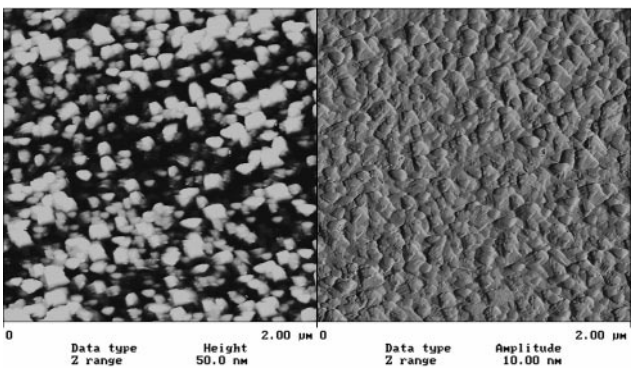

Fig. 10 Tapping mode AFM top view of the precipitates formed hydrothermally. The two views are in height (left) and in amplitude mode (right).

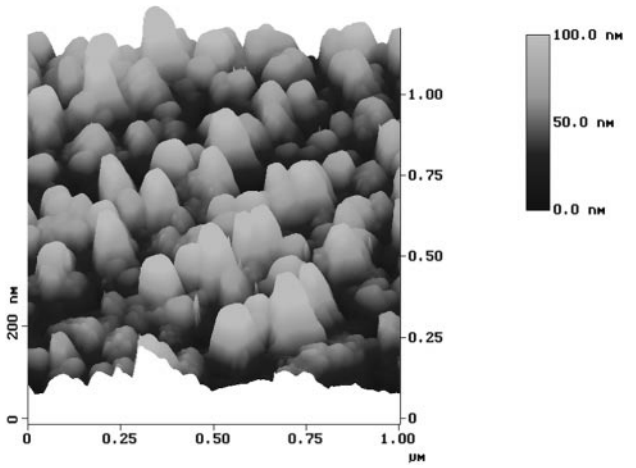

Fig. 11 A surface view of a typical Zr/DBP substrate after the formation of hematite crystallites under hydrothermal conditions.

displayed in Fig. 11 shows the particles to have a rounded morphology. The particles range extend up to 100 nm in height and 50 to 150 nm in lateral extent. It must be noted that the height can only be estimated assuming that the flat portions of the image correspond to the substrate. Owing to the manner in which the images are acquired in tapping-mode AFM, it is difficult to decide whether the crystals are faceted. Fig. 10 indicates however that the crystals seem to grow with a preferential direction, being hemispheroidal in shape with the short axis perpendicular to the plane of the substrate. The crystals are also seen to taper down towards the tips. The heights are not as uniform as the extent of the crystals in the plane of the substrate. We have not been able to verify so far whether this direction is that of the *c* axis as suggested from the discussion of the structure.

4 Conclusion

We have demonstrated through surface plasmon spectroscopy, the stability of Zr–phosphonate multilayers (more than three layers). The termination of the multilayer with phosphonate groups seems to induce the growth of hematite films under the conditions in which hematite powders are normally prepared. That the material deposited is hematite has been confirmed through Mössbauer spectroscopy and powder X-ray diffraction. Our use of phosphonate multilayer films adds to and complements the work of Bein and coworkers[5,6] in pointing to their use as chemically specific templates that retain their specificity even under rather harsh conditions. While hematite is an important iron oxide, and its preparation as films is of some importance, we suggest that the methods presented here can be extended to the preparation of many other oxide materials as films under hydrothermal conditions. The chief issue is the nature of the termination on the multilayer (*i.e.* the functional group that forms the organic–inorganic interface) and the occurrence and establishment of specific modes of templating at the interface.

Acknowledgements

We are grateful to Professor H.-J. Butt for generous access to his AFM facilities, and to Professor W. Knoll for the SPS apparatus. Financial support from the Fonds der chemischen Industrie is acknowledged. Comments from an anonymous referee have helped greatly.

References

1 B. J. Tarasevich, P. C. Rieke and J. Liu, *Chem. Mater.*, 1996, **8**, 292; P. C. Rieke, B. D. Marsh, L. L. Wood, B. J. Tarasevich,

J. Liu, L. Song and G. E. Fryxell, *Langmuir*, 1995, **11**, 31; P. C. Rieke, B. Tarasevich, L. Wood, M. Engelhard, D. Baer, G. Fryxell, C. John and D. Laken and M. Jaehning, *Langmuir*, 1994, **10**, 619.
2 M. Nagtegaal, P. Stroeve, J. Ensling, P. Gütlich, M. Schurrer, H. Voit, J. Flath, J. Käshammer, W. Knoll and W. Tremel, in preparation.
3 C. D. Bain, E. B. Troughton, Y.-T. Tao, J. Evall, G. M. Whitesides and R. G. Nuzzo, *J. Am. Chem. Soc.*, 1989, **111**, 321.
4 H. Lee, L. J. Kepley, H. G. Hong and T. E. Mallouk, *J. Am. Chem. Soc.*, 1988, **110**, 618.
5 S. Feng and T. Bein, *Nature*, 1994, **368**, 834.
6 Y. Yan and T. Bein, *J. Phys. Chem.*, 1992, **96**, 9387.
7 E. Matijevic, *Pure Appl. Chem.*, 1980, **52**, 1179.
8 Q. W. Chen, Y. T. Qian, H. Qian, Z. Y. Chen, W. B. Wu and Y. H. Zhang, *Mater. Res. Bull.*, 1995, **30**, 443.
9 R. M. Cornell and U. Schwertmann, *The Iron Oxides*, VCH, Weinheim, 1996.
10 J. K. Lin, J. M. Sivertsen and J. H. Judy, *IEEE Trans. Magn.*, 1986, **22**, 50.
11 S. Joshi, R. Nawathey, V. N. Koinkar, V. P. Godbole, S. M. Chaudhari and S. B. Ogale, *J. Appl. Phys.*, 1988, **64**, 5467.
12 M. Langiet, M. Labeau and J. C. Joubert, *IEEE Trans. Magn.*, 1986, **22**, 600.
13 Y. T. Qian, C. M. Niu, C. Hannigan, S. Yang, K. Dwight and A. Wold, *J. Solid State Chem.*, 1991, **92**, 20.
14 H. Wolf, PhD Thesis, Universität Mainz, 1995.
15 H. Lee, L. J. Kepley, H.-G. Hong, S. Akther and T. E. Mallouk, *J. Phys. Chem.*, 1988, **92**, 2597.
16 T. M. Putvinski, M. L. Schilling, H. E. Katz, C. E. D. Chidsey, A. M. Mujsce and A. B. Emerson, *Langmuir*, 1990, **9**, 1567.
17 B. L. Frey, D. G. Hanken and R. M. Corn, *Langmuir*, 1993, **6**, 1815.
18 H. E. Katz, G. Scheller, T. M. Putvinski, M. L. Schilling, W. L. Wilson and C. E. D. Chidsey, *Science*, 1991, **254**, 1485.
19 W. Knoll, *Mater. Res. Bull.*, 1991, **16**, 29.
20 H. Raether, *Surface Plasmons on Smooth and Rough Surfaces and on Gratings*, Springer Tracts in Modern Physics 111, Springer Verlag, Berlin, 1988.
21 T. R. Lee, R. I. Carey, H. A. Biebuyck and G. M. Whitesides, *Langmuir*, 1994, **10**, 741.
22 A. N. Christensen, P. Convert and M. S. Lehmann, *Acta Chem. Scand.*, *Sect. A*, 1980, **34**, 771.
23 J. Dousma and P. L. Bruyn, *J. Colloid Interface Sci.*, 1976, **56**, 527.
24 N. J. Reeves and S. Mann, *J. Chem. Soc.*, *Faraday Trans.*, 1991, **87**, 3875.
25 XND version 1.17, J.-F. Bérar, European Synchrotron Radiation Facility, Grenoble, France, 1998.
26 H. D. Megaw, *Crystal Structures: A Working Approach*, W. B. Saunders, Philadelphia, 1972.
27 A. Ulmann, *Chem. Rev*., 1996, **96**, 1533.

Paper 8/09319I